# High-selectivity palladium catalysts for the partial hydrogenation of alkynes by gas-phase cluster deposition onto oxide powders

Peter R. Ellis, Christopher M. Brown, Peter T. Bishop, Dmitrij Ievlev, Jinlong Yin, Kevin Cooke & Richard E. Palmer

View supplementary material 🗗

Published online: 20 Jul 2018.

Submit your article to this journal 🗗

Article views: 18

View Crossmark data 🗗

Taylor & Francis
Taylor & Francis Group

# High-selectivity palladium catalysts for the partial hydrogenation of alkynes by gas-phase cluster deposition onto oxide powders

Peter R. Ellis [a], Christopher M. Brown[a], Peter T. Bishop[a], Dmitrij Ievlev[b], Jinlong Yin[b], Kevin Cooke[b] and Richard E. Palmer [c]

[a]Johnson Matthey, Blount's Court, Sonning Common, Reading, UK; [b]Teer Coatings Ltd., Miba Coating Group, West Stone, Berry Hill Industrial Estate, Droitwich, Worcestershire, UK; [c]College of Engineering, Swansea University, Bay Campus, Swansea, UK

## ABSTRACT

The selective hydrogenation of alkynes is an important reaction in the synthesis of fine and bulk chemicals. We show that the synthesis of metal nanoparticles in the gas phase, followed by deposition onto conventional support powders results in materials that perform as well as those made by typical methods for making catalysts (impregnation, deposition). The nature of the active sites in these catalysts is explored.
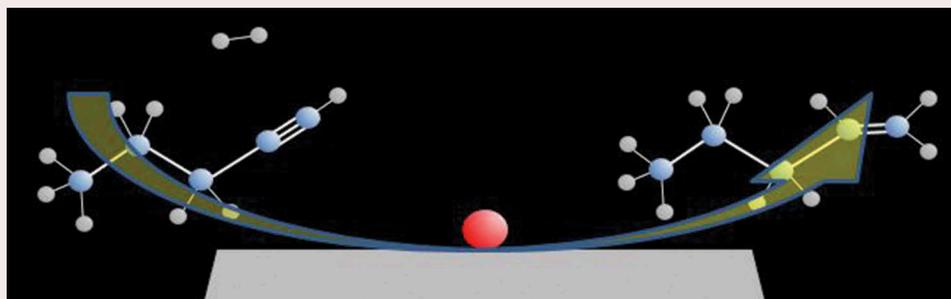
## Introduction

The selective hydrogenation of a range of substrates is a key technology in both the bulk and fine chemicals industries [1]. In both contexts, selectivity to the desired product is usually a key attribute: loss of reagent to the formation of undesired products is economically undesirable and can lead to challenges in separation downstream. This means that there is a pressing need for more selective catalysts and processes for a range of selective hydrogenation reactions. One way to meet this need is the design and realization of catalytic materials with improved properties. The majority of commercial catalysts are made using a small number of synthesis methods (impregnation, precipitation, solid-state methods, etc.). There is good reason for this: they are reliable, economic, and can be performed at the necessary scale for commercial use. However, they are not always able to produce materials that are truly optimized.

Making an optimized catalyst requires control over the synthesis of the active site, as well as attachment of the active site to the catalyst support (which is typically needed for mechanical properties as well as to disperse the active sites). For the former, the use of nanoparticles synthesized in solution is an attractive proposition. They can be produced ex situ from the catalyst support by controlling the key properties such as particle size [2], shape [3], and the nature of the exposed surfaces [4] and can contain more than one metal with controlled location (such as a core–shell structure) [5]. Attaching these particles to supports is a complex process. Although in some cases the presence of stabilizers has been shown to be beneficial [6], often the stabilizers need to be removed for optimal performance. Ligand removal often changes the nature of the nanoparticle, for example through a loss of size control [7], rendering them poorly performing. Ligand removal has been addressed in a few selected cases, for example in a catalyst made with polymer-stabilized nanoparticles [8], but significant progress is still needed to find a general method that would allow manufacturing at scale to take place.

Synthesis of nanoparticles by aggregation of metal atoms or ions in the gas phase is a promising technology [9] that addresses many of these issues. In a typical configuration, atoms are generated from a metal source and these are condensed to form

clusters. Typically, some of the particles formed are charged, which allows them to be manipulated using applied voltages, mass-selected if desired, and finally guided onto the support. The technique can offer particle-size control from less than 2 nm to over 10 nm [10] and also some control over the interaction between the nanoparticle and the support: the accelerating voltage can be used to control the impact of the particle into the support [11–13]. We [14] and others [15] have, in this way, made bimetallic clusters from a number of metals. Yang et al. [16] have demonstrated the selective deposition of silver clusters onto the top face of silicon pillars. A combination of these different features should allow the design of catalysts with a high degree of control.

In this work, we use gas-phase cluster deposition as a method to deposit size-controlled palladium nanoparticles onto two typical commercial powder support materials. We employ the selective partial hydrogenation of 1-pentyne (Scheme 1) as a model reaction for the selective hydrogenation of alkynes relevant to both the bulk [17] and fine [18,19] chemicals industries. We have previously reported the good performance of a palladium catalyst prepared by gas-phase cluster deposition onto a flat graphite tape as a catalyst for the selective hydrogenation of 1-pentyne [20], and we have also observed changes in the atomic structure of size-selected palladium nanoparticles during this reaction [21]. Most recently, we have reported the performance of PdM bimetallic cluster catalysts in alkyne hydrogenation [14]. In this paper, we describe the performance of catalysts prepared by gas-phase nanoparticle synthesis in selective alkyne hydrogenation and offer some perspective on the nature of the reactive sites.

incipient wetness impregnation, deposition-precipitation, and ion-exchange methods. Details of the methods used are presented in the Supporting Information. Table 1 compares the properties of the catalysts. The palladium content of the materials is low at 0.1wt%. This was driven by the experimental configuration for gas-phase cluster deposition. However, the efficient use of scarce precious metal resources is a key consideration, and synthetic methods for making good catalysts at these low loadings are valuable. Figure 1 shows representative TEM images of the catalysts synthesized by gas-phase cluster deposition, whereas images of the other catalysts are presented in Fig. S2. Table 1 lists the particle-size ranges for the catalysts. It was difficult to determine precise distributions of the nanoparticles due to clustering in some systems and low loading in the others.

In gas-phase cluster deposition on both supports, nanoparticles are observed only close to the support surface, where they often form agglomerates. In the case of titania, the support is present as a loose agglomerate of 20–30 nm particles, and the palladium particles are deposited on the surface of these agglomerates. The alpha alumina is present as much larger particles (20–40 μm), and here the palladium nanoparticles are deposited on the alumina particle surface with little transport of the nanoparticles into the interior of the alumina. Although deposition on the external surface is a general feature of gas-phase cluster deposition processes, neither the alpha alumina nor the titania used in this work is significantly porous, so the materials are all expected to be surface enriched in palladium. Clearly, this would not be the case for a more porous support, such as a typical gamma alumina.

## Results and discussion

### Catalyst synthesis

Palladium was deposited on two conventional support powders (alpha alumina and titania) to make representative catalysts for the vapor-phase selective hydrogenation of 1-pentyne to 1-pentene. Catalysts were prepared by four methods: gas-phase cluster beam deposition,

### Catalyst testing

The catalysts' performance in the selective hydrogenation of 1-pentyne (Scheme 1) were tested in a quartz microreactor using the as-prepared powders. 1-pentyne vapor and a hydrogen–helium mixture were flowed through a catalyst bed while the temperature was increased from ambient to 250°C. Full details of the catalytic testing
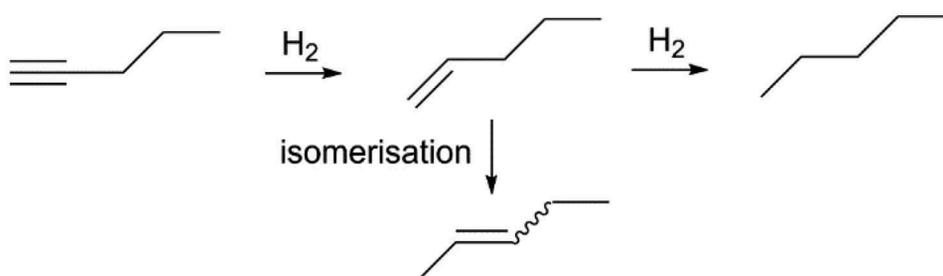


**Scheme 1.** The selective hydrogenation of 1-pentyne to 1-pentene and two competing reactions: further hydrogenation to pentane and isomerization of the double bond to give cis and trans-2-pentene.
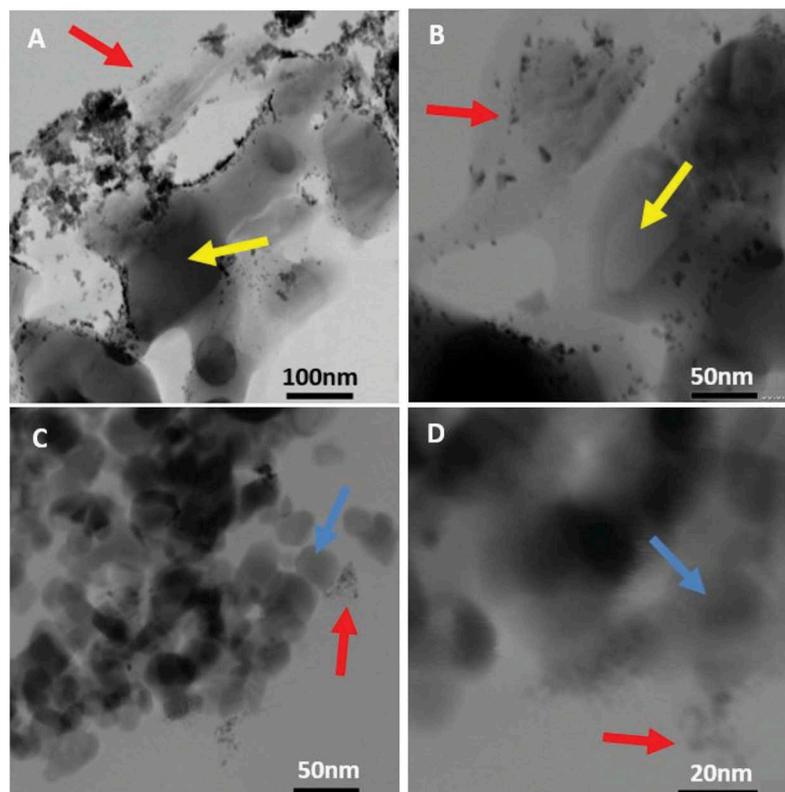
**Figure 1.** Representative bright-field aberration-corrected STEM images of the catalysts prepared by gas-phase cluster deposition: (A)–(B) Pd/α-Al$_2$O$_3$; (C)–(D) Pd/TiO$_2$. Examples of palladium particles are indicated by red arrows, alpha alumina particles with yellow arrows, and titania particles with blue arrows.

methodology are presented in the Supporting Information. Figure 2 shows the performance of the eight catalysts when tested at equivalent palladium content and bed depth. None of the catalysts showed a significant amount of activity at low temperature (<50° C). As the temperature increases above this temperature, the 1-pentyne conversion increases. The most active of the catalysts studied were Pd/α-Al$_2$O$_3$ prepared by impregnation and by deposition-precipitation. The gas-phase cluster deposition materials were the least active, but also the most selective, with combined selectivity to 2-pentenes and pentane of less than 10% across the temperature range studied.

Given the difference in activity between the GCD and reference catalysts, it was of interest to compare their performance at close to iso-conversion. This was
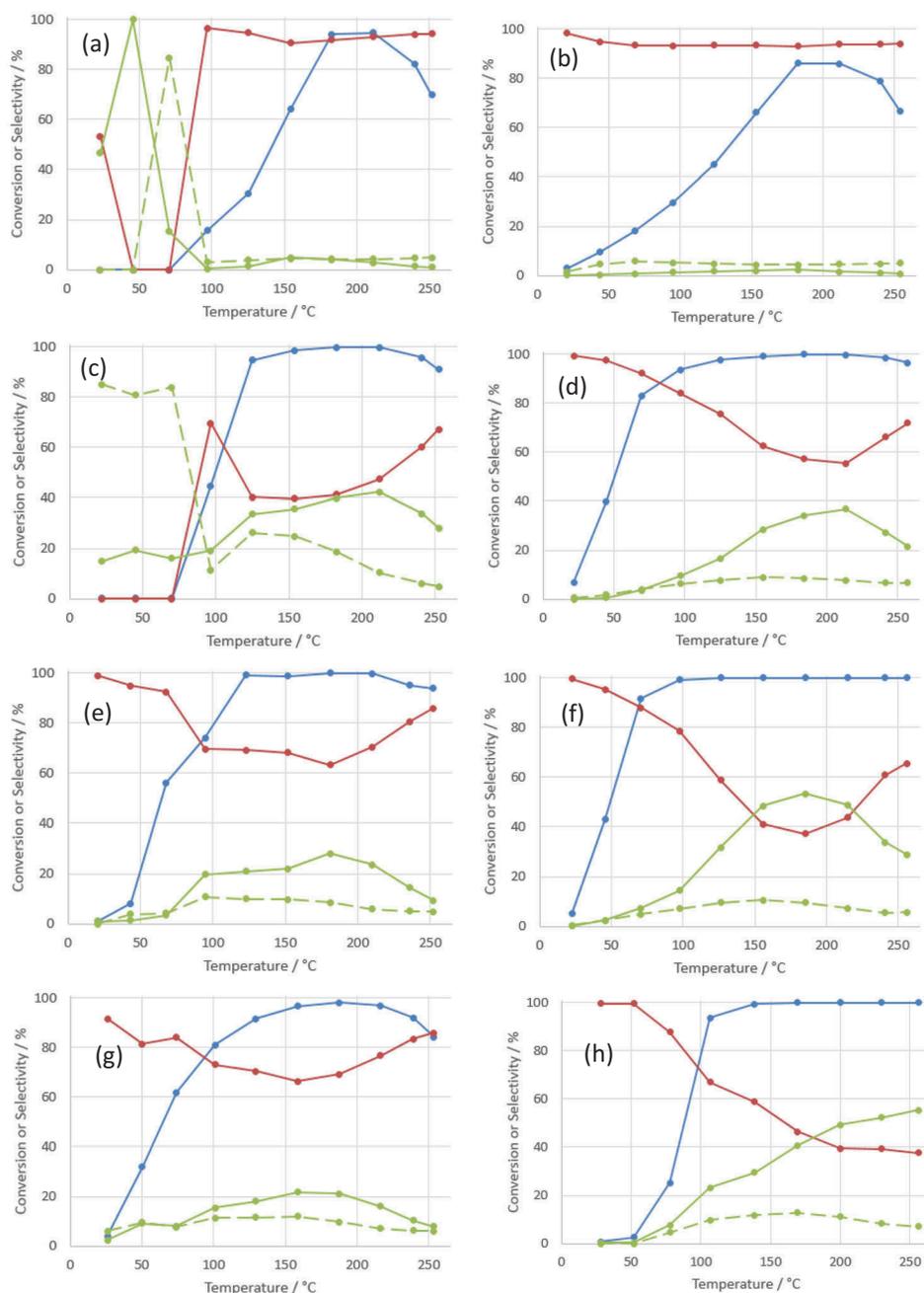
achieved by varying the catalyst mass at constant flow rates of hydrogen and 1-pentyne. Details of the procedure are presented in the Supporting Information. Table 2 shows the selectivity of each catalyst when the temperature was at a point where 80% conversion was achieved (T$_{80}$). Under these conditions, the selectivity of the catalysts is much closer, although the GDC catalysts are still among the best for each support studied. The most selective catalysts are Pd/α-Al$_2$O$_3$ prepared by impregnation, deposition-precipitation, and gas-phase cluster deposition with over 90% selectivity to 1-pentene. The Pd/TiO$_2$ catalysts are generally less selective. Intriguingly, the two catalysts prepared by the ion-exchange method have very similar performances.

It is clearly of interest to understand the origin of the performance of the eight catalysts studied. The materials present a range of metal–support interaction types, and these can be used to understand how the nature of the active site affects catalytic performance. For the materials prepared by gas-phase cluster deposition, there is no contact between Pd$^{2+}$ ions and the support, whereas for ion-exchange materials, the interaction is governed by the adsorption of Pd$^{2+}$ ions onto reactive sites on the support, such as Al-O$^-$ or Ti-O$^-$, by the replacement of two H$^+$ ions with one Pd$^{2+}$ ion. The isoelectric points of alpha alumina and titania are reported to be pH 9.3 [22] and pH 5.4 [23], respectively. The metal precursor used in this study, palladium

**Table 1.** Palladium content (ICP-ES) and particle-size range (TEM) for the catalysts studied.

| Catalyst | Synthesis Method | Pd content/ wt.% | Pd particle size/ nm |
|---|---|---|---|
| Pd/α-Al$_2$O$_3$ | Gas-phase cluster deposition | 0.3 | 3–8[a] |
| | Impregnation | 0.13 | 2–6 |
| | Deposition-precipitation | 0.14 | 2.5–5.5 |
| | Ion exchange | 0.04 | 1–2 |
| Pd/TiO$_2$ | Gas-phase deposition | 0.18 | 4–6 |
| | Impregnation | 0.13 | 1–3 |
| | Deposition-precipitation | 0.13 | 1.5–3.5 |
| | Ion exchange | 0.53 | 1–6 |

[a]Larger particles are also observed from the coalescence of the primary particles.

**Figure 2.** Catalyst testing in 1-pentyne hydrogenation. The 1-pentyne conversion is shown in blue, with selectivity to 1-pentene (red), 2-pentenes (green, solid line), and pentane (green, solid line) also shown. The catalysts are (a) Pd/TiO$_2$ GCD; (b) Pd/α-Al$_2$O$_3$ GCD; (c) Pd/TiO$_2$ impregnation; (d) Pd/α-Al$_2$O$_3$ impregnation; (e) Pd/TiO$_2$ deposition-precipitation; (f) Pd/α-Al$_2$O$_3$ deposition-precipitation; (g) Pd/TiO$_2$ ion exchange; and (h) Pd/α-Al$_2$O$_3$ ion exchange.

**Table 2.** Comparison of the catalytic performance at 80% 1-pentyne conversion. T$_{80}$ is the temperature at which 1-pentyne conversion reached 80%.

| Synthesis Method | T$_{80}$/°C | Selectivity/% | | |
|---|---|---|---|---|
| | | 1-pentene | 2-pentenes | pentane |
| **Pd/alpha alumina** | | | | |
| Impregnation | 68 | 93 | 3 | 4 |
| Deposition-Precipitation | 65 | 90 | 6 | 4 |
| Ion Exchange | 101 | 71 | 20 | 9 |
| Gas-Phase Deposition | 101 | 93 | 2 | 5 |
| **Pd/titania** | | | | |
| Impregnation | 116 | 49 | 29 | 22 |
| Deposition-Precipitation | 101 | 69 | 20 | 11 |
| Ion Exchange | 99 | 74 | 15 | 11 |
| Gas-Phase Deposition | 120 | 73 | 18 | 9 |

nitrate, is acidic, which makes the impregnating solution acidic. However, even at lower pH, some negatively charged surface sites will exist [24]; clearly, the number and distribution will be affected by the nature of the palladium precursor solution and the support material. At ion-exchange sites, palladium will be transformed during subsequent thermal treatments (in this work, drying at 100°C and hydrogen reduction at 250°C). In the final catalyst, they will behave differently from the main nanoparticulate palladium phase and invariably lead to some loss of selectivity under reaction conditions. If these sites were highly active, as might be

anticipated for a very well-dispersed phase, they could influence selectivity disproportionately.

The presence of palladium on both supports shows that ion exchange has occurred. The particle-size range of the ion-exchange catalyst is similar to the other methods of preparation investigated, although the size of the smallest particles observed is somewhat lower (typically 1 nm). It is challenging to detect supported palladium particles by TEM without aberration correction if the diameter is less than 1 nm [25], so the presence of particles smaller than 1 nm in our materials is possible. The $Pd/TiO_2$ catalyst prepared by ion exchange has the broadest particle-size range of all of the materials studied, whereas the corresponding $Pd/\alpha\text{-}Al_2O_3$ has a very tight particle-size distribution. This shows that the nature of the support influences the fate of the ion-exchanged species during catalyst synthesis. ICP measurements show that there is much more palladium present on the titania support than on the alpha alumina after the ion-exchange process. This is a consequence of the surface chemistry of the two supports [22, 26]. The higher palladium content of the $Pd/TiO_2$ prepared by ion exchange leads to larger nanoparticle formation, most likely by sintering during the reduction process. Both the ICP and TEM results are in agreement with modeling studies, which show that the metal–support interaction is very important in determining how particles grow on the support surface [27].

A second reactive site that is relevant is the interface between the metal particle and the support (such as Al-O-Pd or Ti-O-Pd) where the palladium is not reduced. These sites occur where the palladium nanoparticle meets the support and are often poorly defined. Yet, some interfacial interactions are known to be strong, for example stabilizing small particles even at high temperatures [28]. Interfacial sites are known to be critical for good performance in some catalytic reactions, including CO oxidation over palladium catalysts [29], but they also have the potential to perform undesirable side-reactions in the same way as the ion-exchange sites described above. All the catalysts prepared by chemical methods (impregnation, deposition-precipitation, and ion exchange) might be expected to have M-O-Pd sites (M = Al, Ti) at the interface between the palladium nanoparticles and the support. Such interfacial sites are known to be highly active in CO oxidation [29]. If this is the case, catalysts prepared by chemical routes might be expected to give better catalysts in CO oxidation testing than the catalysts prepared by gas-phase deposition. We tested this idea by measuring the activity of the set of catalysts in CO oxidation. Full details of this are presented in the Supporting Information; the performance is summarized in Table 3.

The results of CO oxidation testing show interesting trends. The $Pd/TiO_2$ materials follow the trend we expected: the gas-phase deposition catalyst has the highest $T_{50}$ value (is the least active) and the other catalysts,

**Table 3.** Results of CO oxidation testing. $T_{50}$ is the temperature at which half the CO is converted.

| Catalyst | Synthesis Method | $T_{50}$/°C |
|---|---|---|
| $Pd/\alpha\text{-}Al_2O_3$ | Impregnation | 180 |
| | Deposition | 181 |
| | Ion Exchange | 185 |
| | Gas-Phase Deposition | 194 |
| $Pd/TiO_2$ | Impregnation | 206 |
| | Deposition | 117 |
| | Ion Exchange | 114 |
| | Gas-Phase Deposition | 231 |

which might be expected to contain the most interfacial (and ion exchange) sites, have lower $T_{50}$ values (more active). However, the $Pd/\alpha\text{-}Al_2O_3$ catalysts all had similar $T_{50}$ values. This indicates that the number or nature of interfacial sites is sensitive to the nature of the support. The interaction between the palladium and the alpha alumina support is rather weak. However, when the metal–support interaction is appreciable, as in the case of palladium and the titania support, it does influence the reactivity of the catalyst.

The different chemical natures of the two supports will also influence the catalysis. Alpha alumina is a highly crystalline material with micron-sized particles, a low surface area (10 $m^2$ $g^{-1}$), and little porosity. Its surface contains little functionality, and as such it is often difficult to disperse metals, especially at higher loadings [30]. The titania support studied, on the contrary, consists of micron-sized agglomerates of loosely held 20–40 nm nanoparticles. These have little porosity, but the gaps between the nanoparticles can act as pores in certain situations. In contrast to alpha alumina, palladium can interact strongly with titania through the well-known SMSI effect [31].

The influence of the support can be seen in the catalysis data in Table 2. The most selective catalysts are based on alpha alumina, and this reflects the inert nature of the support; ion-exchanged sites are few (as shown by the low palladium content of the ion-exchanged $Pd/\alpha\text{-}Al_2O_3$ catalyst) and the interfacial sites are less active: reduction of palladium is not inhibited by a strong interaction with the support. The lower selectivity of the $Pd/TiO_2$ catalysts is, in turn, a consequence of their more reactive nature, which stabilizes $Pd^{2+}$ against reduction.

One factor that has been found to affect palladium-catalyzed selective alkyne hydrogenation is the formation of palladium hydride and carbide phases. Palladium hydride phases are known to form readily when reduced palladium catalyst nanoparticles are exposed to hydrogen [32] and can hydrogenate alkenes even in the absence of gaseous hydrogen [33]. The presence of subsurface hydrogen has been found to allow hydrogenation and dehydrogenation reactions to occur more readily than systems where subsurface hydrogen is not accessible [34]. The thermal stability of palladium hydride is limited [35] even in the presence of hydrogen, such as in our system, and also is less stable in smaller nanoparticles [35] whereas more surface

hydrogen can be formed due to the larger available surface area [36]. Hence, it seems that the presence of bulk palladium hydride is not a major factor at temperatures where good catalytic performance is observed (T > 50°C for all catalysts). Tew *et al.* observed the formation of a carbide-like phase of palladium on the exposure of reduced catalysts to 1-pentyne [32]. This was a more stable phase than palladium hydride, and re-exposure to hydrogen did not change the palladium carbide structure appreciably. The formation of palladium carbide was found to be independent of palladium particle size [37] and also to be suppressed at $H_2$/1-pentyne ratios above 10. Our $H_2$/1-pentyne ratio is of the order of 60, and so the presence of palladium carbide phases is unlikely. The factors that affect the amount and nature of palladium carbide formation are not completely understood; it is possible that the formation of palladium carbide species is a characteristic of a good selective hydrogenation catalyst.

To assess the durability of the catalysts made in 1-pentyne hydrogenation, they were retested using a modified hydrogenation protocol (see the Supporting Information). Once the temperature had been increased to its maximum value, 240°C, the flow was maintained at that temperature for a further three hours. Thus, deactivation and changes in selectivity could be observed. Figure 3 summarizes the performance of the catalysts at the end of the three-hour dwell period and shows the changes of selectivity over that time. For both Pd/TiO₂ and Pd/α-Al₂O₃ systems, the most selective catalysts were those prepared by the gas-phase cluster deposition method. They showed

good selectivity at the start of the dwell period, which improved in the first part of the experiment and was then stable. The improvement was much quicker for Pd/α-Al₂O₃ (< 20 min) than for Pd/TiO₂ (60 min). For the Pd/α-Al₂O₃ system, the catalysts prepared by the conventional methods are much less selective, and the selectivity did not change during the experiment. In the Pd/TiO₂ system, meanwhile, the impregnated catalyst is poorly selective, but the materials prepared by deposition-precipitation and impregnation show reasonable selectivity. The selectivity shown by all three catalysts improved over time, although the catalyst prepared by gas-phase cluster deposition was still the most selective. The stability of the gas-phase cluster deposition catalysts during the reaction at 240°C shows that the nanoparticles do not change significantly with time. If sintering was occurring, changes in activity and selectivity would be expected.

The selectivity of the Pd/α-Al₂O₃ catalysts varied much less than that of the Pd/TiO₂ catalysts. One difference between alpha alumina and titania is the reducibility. Palladium is known to be able to reduce titania with hydrogen at temperatures lower than those used here [38,39], which could lead to changes in some of the active sites. It is possible that a slow deactivation of the unselective sites is responsible for the improved selectivity observed here.

The nature of the nanoparticles in the gas-phase cluster deposition catalysts is strongly influenced by the lack of contact between Pd(II) and the support, unlike impregnation, deposition-precipitation, or ion-
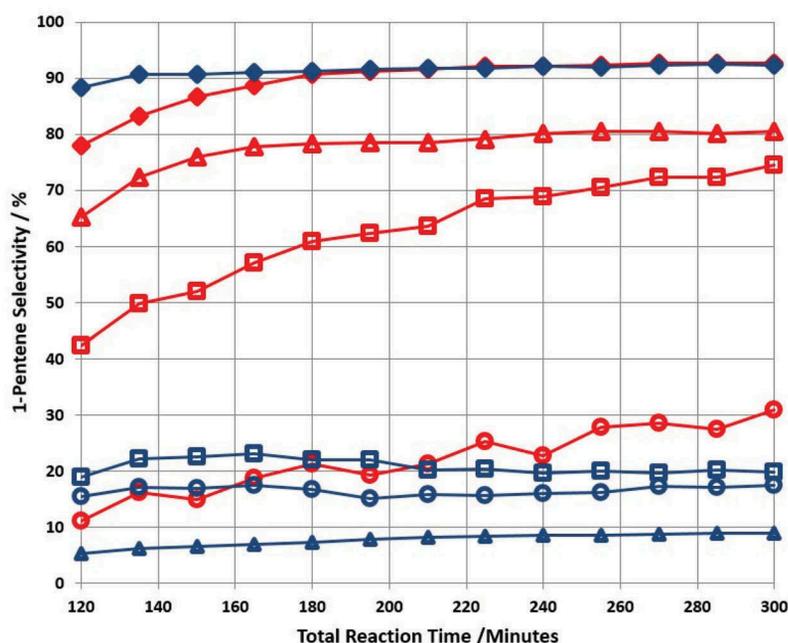


**Figure 3.** Comparison of catalytic performance in the selective hydrogenation of 1-pentyne to 1-pentene during extended operation at a fixed temperature, 240°C. The chart shows Pd/α-Al₂O₃ (blue) and Pd/TiO₂ (red) catalysts prepared by gas-phase cluster deposition (diamonds), deposition precipitation (squares), impregnation (circles), or ion exchange (triangles). The table summarizes the 1-pentyne conversion and 1-pentene selectivity after a dwell time of 180 min.

exchange processes. Better performance than the ion-exchanged materials in 1-pentyne hydrogenation and the lack of activity in CO oxidation suggest an absence of Pd-O-Al and Pd-O-Ti sites in Pd/Al$_2$O$_3$ and Pd/TiO$_2$, respectively. These sites, therefore, appear to be responsible for the formation of 2-pentene isomers.

The structure of the gas-phase cluster deposition catalysts therefore seems likely to contain metallic nanoparticles anchored strongly enough to the support to prevent sintering (since performance is maintained in 1-pentyne hydrogenation with an extended reaction time). The anchoring force seems likely to feature a role for surface defect sites, as has been reported for Pd [40], Pt [41], and Au [42] catalysts previously. Work is ongoing to understand this interaction more completely.

## Conclusions

The synthesis of catalysts by methods such as gas-phase cluster deposition allows control of the properties of metal nanoparticles, with little or no dependence on the support properties. In this paper, we have demonstrated that palladium catalysts prepared by a gas-phase cluster deposition method can be as active and selective in the selective hydrogenation of alkynes as materials prepared by conventional methods. This is observed for both support materials studied here (TiO$_2$ and α-Al$_2$O$_3$). The particle sizes of all the materials studied here are similar, so this is not a particle-size effect. Catalysts prepared by the gas-phase cluster deposition method contain less-active interfacial sites, as shown by their lower activity in CO oxidation.

## Disclosure statement

No potential conflict of interest was reported by the authors.

## ORCID

Peter R. Ellis http://orcid.org/0000-0002-2806-7915
Richard E. Palmer http://orcid.org/0000-0001-8728-8083

## References

[1] Vilé G, Albani D, Almora-Barrios N, et al. Advances in the design of nanostructured catalysts for selective hydrogenation. Chem Cat Chem. 2016;8:21–33.

[2] Baeza JA, Calvo L, Gilarranz MA, et al. Catalytic behavior of size-controlled palladium nanoparticles in the hydrodechlorination of 4-chlorophenol in aqueous phase. J Catal. 2012;293:85–93.

[3] Shao M, Odell J, Humbert M, et al. Electrocatalysis on shape-controlled palladium nanocrystals: oxygen reduction reaction and formic acid oxidation. J Phys Chem C. 2013;117:4172–4180.

[4] Zhang J, Feng C, Deng Y, et al. Shape-controlled synthesis of palladium single-crystalline nanoparticles: the effect of HCl oxidative etching and facet-dependent catalytic properties. Chem Mater. 2014;26:1213–1218.

[5] Henning AM, Watt J, Miedziak PJ, et al. Taylor SH and Tilley RD, volcano-like behavior of Au-Pd core-shell nanoparticles in the selective oxidation of alcohols. Angew Chem Intl Edn. 2013;52:1477–1480.

[6] Albani D, Vilé G, Mitchell S, et al. Ligand ordering determines the catalytic response of hybrid palladium nanoparticles in hydrogenation. Catal Sci Technol. 2016;6:1621–1631.

[7] Menard LD, Xu F, Nuzzo RG, et al. Preparation of TiO$_2$-supported Au nanoparticle catalysts from a Au13 cluster precursor: ligand removal using ozone exposure versus a rapid thermal treatment. J Catal. 2006;243:64–73.

[8] Lopez-Sanchez JA, Dimitratos N, Hammond C, et al. Facile removal of stabilizer-ligands from supported gold nanoparticles. Nature Chemistry. 2011;3:551–556.

[9] Grammatikopoulos P, Steinhauer S, Vernieres J, et al. Nanoparticle design by gas-phase synthesis. Adv Phys.: X. 2016;1:81–100.

[10] Perez-Alonso FJ, McCarthey DN, Nierhoff A, et al. The effect of size on the oxygen electroreduction activity of mass-selected platinum nanoparticles. Angew Chem Intl Edn. 2012;51:4641–4645.

[11] Palmer RE, Pratontep S, Boyen H-G. Nanostructured surfaces from size-selected clusters. Nat Mater. 2003;2:443–448.

[12] Carroll SJ, Nellist PD, Palmer RE, et al. Shallow implantation of "size-selected" Ag clusters into graphite. Phys Rev Lett. 2000;84:2654.

[13] Pratontep S, Preece P, Xirouchaki C, et al. Scaling relations for implantation of size-selected Au, Ag, and Si clusters into graphite. Phys Rev Lett. 2003;90:055503.

[14] Ellis PR, Brown CM, Bishop PT, et al. The cluster beam route to model catalysts and beyond. Faraday Discuss. 2016;188:39–56.

[15] Law YT, Doh WH, Luo W, et al. Study of ethanol reactivity over Ni, Co and NiCo-ZnO Model Catalysts. J Mol Catal A: Chemical. 2014;381:89–98.

[16] Yang Q, Joyce DE, Saranu S, et al. A combined approach for deposition and characterization of atomically engineered catalyst nanoparticles. Catalysis, Structure & Reactivity. 2015;1:125–131.

[17] McCue AJ, Anderson JA. Recent advances in selective acetylene hydrogenation using palladium containing catalysts. Front Chem Sci Eng. 2015;9:142–153.

[18] Miyaoka H, Hara Y, Shinohara I, et al. Synthesis and structural revision of marine eicosanoid agardhilactone. Tetrahedron Lett. 2005;46:7945–7949.

[19] Cram DJ, Allinger NL, Macro Rings XIII. Synthesis and properties of 1,7-Cyclododecadiyne and related Compounds. J Am Chem Soc. 1956;78: 2518–2524. Chinchilla R, Nájera C, Chemicals from Alkynes with Palladium Catalysts. Chem. Rev., 2014; 114: 1783-1826.

[20] Habibpour V, Song MY, Wang ZW, et al. Novel powder-supported size-selected clusters for heterogeneous catalysis under realistic reaction conditions. J Phys Chem C. 2012;116:26295–26299.

[21] Hu K-J, Plant SR, Ellis PR, et al. Bishop PT Palmer RE, The effects of 1-pentyne hydrogenation on the atomic structures of size-selected Au N and Pd N (N= 923 and 2057) nanoclusters. Phys Chem Chem Phys. 2014;16:26631–26637.

[22] Veeramasuneni S, Yalamanchili MR, Miller JD. Measurement of interaction forces between silica and alpha-alumina by atomic force microscopy. J Colloid Interf Sci. 1996;184:594–600.

[23] Sun J, Gao L. Development of a dispersion process for carbon nanotubes in ceramic matrix by heterocoagulation. Carbon. 2003;41:1063–1068.

[24] Suttiponparnit K, Jiang J, Sahu M, et al. Role of surface area, primary particle size, and crystal phase on titanium dioxide nanoparticle dispersion properties. Nanoscale Res Lett. 2011;6:27.

[25] Simakova I, Simakova O, Mäki-Arvela P, et al. Deoxygenation of palmitic and stearic acid over supported Pd catalysts: effect of metal dispersion. Appl Catal A: General. 2009;355:100–108.

[26] Cornu D, Petitjohn H, Constantin G, et al. Influence of natural adsorbates of magnesium oxide on its reactivity in basic catalysis. Phys Chem Chem Phys. 2013;15:19870–19878.

[27] Zhang J, Zhang M, Han Y, et al. Nucleation and growth of palladium clusters on anatase $TiO_2$ (101) surface: a first principle study. J Phys Chem C. 2008;112:19506–19515.

[28] Wang W-J, Chen Y-W. Influence of metal loading on the reducibility and hydrogenation activity of cobalt/alumina catalysts. Appl Catal. 1991;77:223–233.

[29] Zhu H, Qin Z, Shan W, et al. Low-temperature oxidation of CO over $Pd/CeO_2$–$TiO_2$ catalysts with different pretreatments. J Catal. 2005;233:41–50.

[30] Eri S, Kinnari KJ, Schanke D, et al., Fischer Tropsch Catalyst, Preparation, and Use Thereof.U.S. Patent 7,351,679 B2 (2008)

[31] Tauster SJ, Fung SC, Garten RL. Strong metal-support interactions. Group 8 noble metals supported on $TiO_2$. J Am Chem Soc. 1978;100:170–175.

[32] Tew MW, Janousch M, Huthwelker T, et al. The roles of carbide and hydride in oxide-supported palladium nanoparticles for alkyne hydrogenation. J Catal. 2011;283:45–54.

[33] Rennard RJ Jr, Kokes RJ. Hydrogenation of ethylene and propylene over palladium hydride. J Phys Chem. 1966;70:2543–2549.

[34] Doyle AM, Shaikhutdinov SK, Freund H-J. Alkene chemistry on the palladium surface: nanoparticles vs single crystals. J Catal. 2004;223:444–453.

[35] Campesi R, Cuevas F, Gadiou R, et al. Hydrogen storage properties of Pd nanoparticle/carbon template composites. Carbon. 2008;46:206–214.

[36] Tew MW, Miller JT, van Bokhoven JA. Particle size effect of hydride formation and surface hydrogen adsorption of nanosized palladium catalysts: $L_3$ edge vs K edge x-ray absorption spectroscopy. J Phys Chem C. 2009;113:15140–15147.

[37] Tew MW, Nachtegaal JM, Huthwelker T, et al. The irreversible formation of palladium carbide during hydrogenation of 1-pentyne over silica-supported palladium nanoparticles: in situ Pd K and $L_3$ edge XAS. Phys Chem Chem Phys. 2012;14:5761–5768.

[38] Shen W-J, Okumara M, Matsumara Y, et al. The influence of the support on the activity and selectivity of Pd in CO hydrogenation. Appl Catal A: General. 2001;213:225–232.

[39] Xu Y, Zhang C, Zhang L, et al. Pd-catalyzed instant hydrogenation of $TiO_2$ with enhanced photocatalytic performance. Energy Environ Sci. 2016;9:2410–2417.

[40] Liu X, Li L, Meng C, et al. Palladium nanoparticles/defective graphene composites as oxygen reduction electrocatalysts: a first-principles study. J Phys Chem C. 2012;116:2710–2719.

[41] Chen J, Wang M, Liu B, et al. Platinum catalysts prepared with functional carbon nanotube defects and its improved catalytic performance for methanol oxidation. J Phys Chem B. 2006;110:11775–11779.

[42] Lopez N, Janssens TVW, Clausen BS, et al. On the origin of the catalytic activity of gold nanoparticles for low-temperature CO oxidation. J Catal. 2004;223:232–235.